CHAPTER 6

Optical Cavity Based Metal (Pd, Au)/ CdSe QDs/ZnO QDs/ ITO Self-Powered Spectrum Selective Photodetectors*

Contentss

*Part of this work is under review:

Hemant Kumar et al. Effects of Optical Resonance on the Performance of Metal (Pd, Au)/CdSe Quantum Dots (QDs)/ ZnO QDs Optical Cavity Based Spectrum Selective Photodiodes. *IEEE Transactions on Electron Devices, (Under Review),* 2018.

CHAPTER 6

Optical Cavity Based Metal(Pd, Au)/ CdSe QDs/ZnO QDs/ ITO Self-Powered Spectrum Selective Photodetectors

6.1 Introduction

We have observed that the inorganic self-powered Au/CdSe QDs/ZnO QDs/n-Si PD (illuminated from the front side) discussed in chapter 4 shows higher responsivity, and detectivity than the hybrid Au/CdSe QDs/PQT-12/ITO self-powered PD (illuminated from backside through the ITO) considered in chapter-5. However, the hybrid self-powered PD of chapter-5 gives much faster rise time and fall time than the inorganic self-powered PD discussed in chapter 4. In this chapter, we will investigate the effect of Schottky metal electrodes on the performance of the back-illuminated metal/CdSe QDs/ZnO QDs/ITO based spectrum selective self-powered PDs for Pd and Au Schottky metals. We have already discussed in chapter-1 that spectrum selective PDs are capable of detecting light in a very narrow spectral width (Um *et al.*, 2011; Qin *et al.*, 2013; Lin *et al.*, 2015; Qiao *et al.*, 2016; Y. Kumar *et al.*, 2017). Contrary to the front-illuminated PD considered in chapter 4, the back side illumination (through the transparent ITO coated glass substrate) in the present case may use 100% illumination area of the active CdSe QDs layer to improve the figure of merit of PD (Baierl *et al.*, 2012). In the proposed PD structure, the ZnO QDs layer acts as the electron transport layer (ETL) as well as a filter layer while the metal (Pd or Au) forms the Schottky contact on the CdSe QDs layer. The device is illuminated from the ITO-substrate side so that the incident light can easily pass through the ZnO QDs ETL cum filter layer to the CdSe QDs layer and the entered light into the CdSe QDs layer is then reflected back

from the metal/CdSe QDs interface into the active CdSe QDs layer again. Since the ZnO has larger bandgap energy than the CdSe, the reflected light from the metal/CdSe QDs interface is also reflected back from the CdSe/ZnO interface into active CdSe layer of the device. As a result, the light entered into the CdSe QDs layer is confined within the active layer for a long time due to multiple reflections from both the metal/CdSe and CdSe/ZnO interfaces which can enhance the absorption as well as responsivity of the device. The effect of reflectance characteristics of light from the metal (Pd, Au)/ CdSe QDs interface on the optical response of the device has been analyzed by both experimentally and theoretically in this chapter. The outline of the present chapter is provided below.

Section 6.2 discusses the fabrication details of the spectrum selective self-powered PD under study. The various measured and theoretical results have been analyzed in details in Section 6.3. Finally, Section 6.4 presents the conclusion and summary of the present chapter.

6.2 Experimental Details

The as-prepared and filtered ZnO-QDs are spin-coated over the cleaned patterned ITO substrates. The ZnO-QDs coated ITO substrates are then heated at 200°C in a prebaked oven for 10-15 mins under ambient environment. This process is repeated until the final thickness of ~260 nm is achieved which is finally verified by using reflectometer (F-20, Filmetrics). The ZnO QDs/ITO substrate is annealed at 250°C under the ambient environment for ~30 mins as already discussed in chapter - 2. The ZnO-QDs layer will act as an electron transport layer (ETL) as well as the filter layer for short wavelength photons. The high thickness of 260 nm of the ZnO QDs is used to

achieve low dark current or noise current for the PD by increasing an inter-electrode separation (Agostinelli *et al.*, 2008; Ng *et al.*, 2008; Ramuz *et al.*, 2008). The ZnO QDs/ITO substrates are placed in spin-coater for deposition of CdSe QDs to act as the active layer of the device as discussed in chapter - 2. The process is repeated until the final thickness of ~80 nm of the CdSe QDs layer is achieved. High purity Au and Pd (99.9%) was deposited by thermal evaporation (HHV, FL400 SMART COAT 3.0 A) accordingly to prepare Au/CdSe QDs/ZnO QDs and Pd/CdSe QDs/ZnO QDs devices. Vacuum deposition of metals was performed at a vacuum of $\sim 10^{-6}$ bar to achieve the thickness of ~80 nm. The rate of the deposition is varied from 0.1 Å/s (< 10 nm) to 1.5 Å/s (>20 nm) to obtain a smooth and uniform deposition. The metal contact is deposited using shadow masking with the area of 0.075 cm^2. The schematic of the fabricated device structure is shown in Figure 6.1 (a).

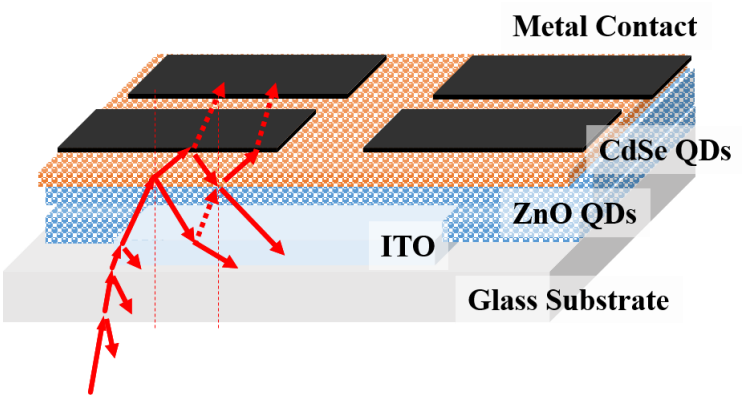

Figure 6.1: Schematic device structure of the spectrum selective self-powered PD depicting reflection from top metal contacts.

6.3 Results and Discussion

In this section, we have presented electrical and photoresponse characteristics of Metal (Pd, Au)/CdSe Quantum Dots (QDs)/ ZnO QDs with theoretical validation.

6.3.1 Electrical Characteristics

The current density (J) vs voltage (V) characteristics of both the Pd/CdSe QDs and Au/CdSe QDs photodiodes measured by using semiconductor parametric analyzer (Agilent B1500A) under dark and illumination of white LED light (96.8 µW/cm^2 at 500 nm) have been shown in Figure 6.2 (a) and (b) respectively.

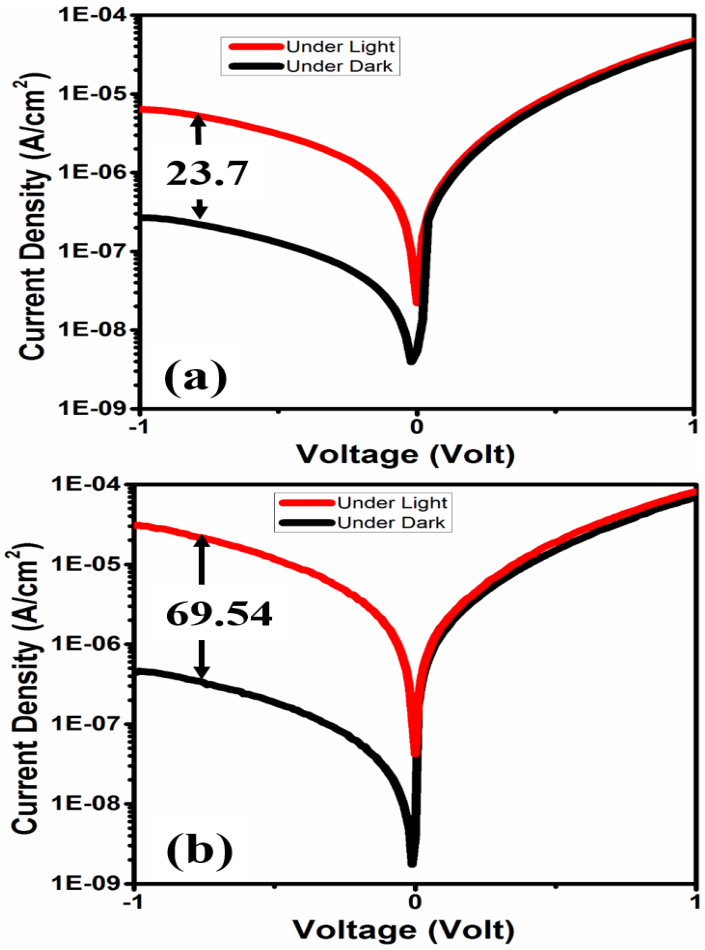

Figure 6.2: (a) J-V characteristics under dark and under light for Schottky photodiode with Au electrode and schematic of device is shown in inset and (b) J-V characteristics under dark and under light for Schottky photodiode with Pd electrode.

The photocurrent density in Pd/CdSe QDs photodiodes is 3.7 times higher than the Au/CdSe QDs based Schottky photodiodes. The rectification ratios (i.e. the ratio of the forward to reverse bias current) of the Au (159) and Pd (157) based devices are

measured to be nearly same. However, the respective contrast ratios (i.e., photocurrent to dark current ratio) of the Pd photodiodes measured at -1 V and 0 V bias voltages are 69.54 and 10.75 which are larger than their corresponding values of 23.7 and 3.33 measured for the Au based photodiodes. The room temperature forward current *(I)*, barrier height ($\phi_{B,eff}$) and the ideality factor (η_i) of the Schottky diodes under study can be calculated under the dark condition by using the following equations (Sze, 2002):

$$I = I_O\left\{= AA^*T^2 \exp\left(-\frac{q\phi_{B,eff}}{kT}\right)\right\}\exp\left(\frac{qV}{\eta_i kT}\right) \tag{6.1}$$

$$\phi_{B,eff} = -\frac{kT}{q}\ln\left(\frac{I_0}{AA^*T^2}\right) \tag{6.2}$$

$$n_i = \frac{q}{kT}\frac{dV}{d\ln(I)} \tag{6.3}$$

where A is the contact area (0.075 cm^2), q is an electronic charge, V is the applied bias, I_0 is the reverse saturation current, T is temperature, k is the Boltzmann constant, and A^* is the Richardson constant (15.6 $Acm^{-2}K^{-2}$ for CdSe). (Tripathi, 2010) The values of forward current *(I)*, barrier height ($\phi_{B,eff}$) and the ideality factor are calculated as 1.89×10^{-8} A, 0.76 V and 2.39 for Au based device and 1.74×10^{-8} A, 0.76 V and 2.36 for the Pd based devices respectively. The capacitance (C) – voltage (V) characteristics represented in terms of the A^2/C^2 vs V curves have been shown in Figure 6.3 (a) and (b) for Au and Pd based devices respectively. To determine the built-in voltage (V_{bi}) and carrier concentration (N_d) in the CdSe QDs layer, the C-V characteristics of the Schottky diodes can be analyzed using Equation 3.1. The built-in voltages are obtained as 0.54 V and 0.41 V whereas the extrinsic carrier concentrations (N_d) are determined as

4.94×10^{16} cm^{-3} and 3.05×10^{16} cm^{-3} for the Au and Pd based photodiodes respectively. The fabricated photodiodes are self-powered and should work with a self-sufficient potential generated within the detector under the effect of illumination.

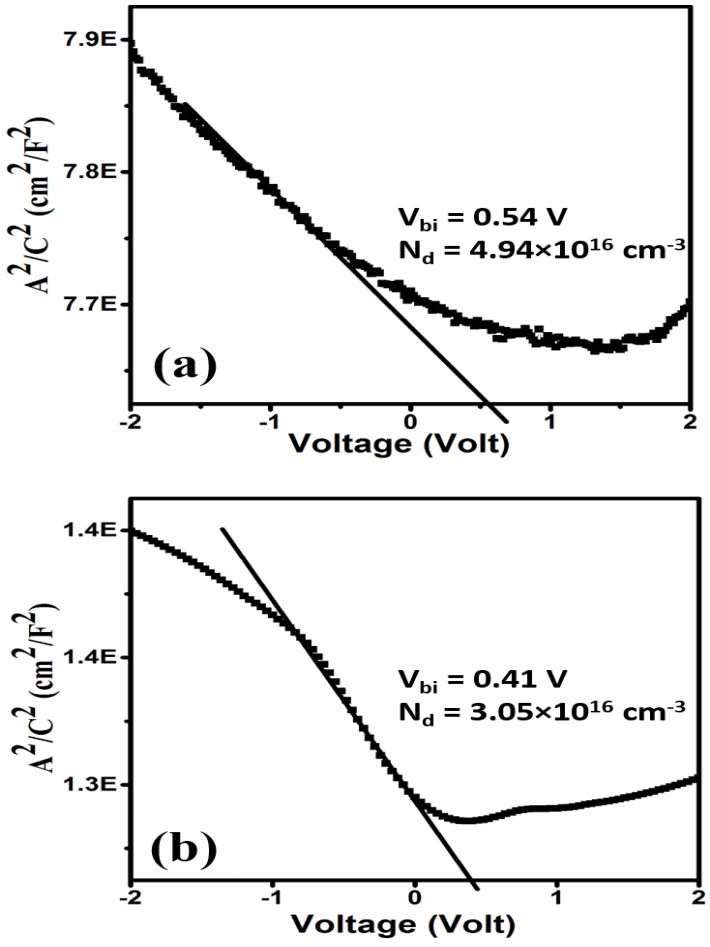

Figure 6.3: (a) Inverse C-V characteristics for Schottky diode with Au electrode and (b) Inverse C-V characteristics for Schottky diode with Pd electrode.

The depletion region in self-powered photodiode plays a vital role in determining the performance of device since the photo-generated carriers of this region under illumination derive the performance of the device as mentioned in chapter 4. The width of the depletion region inside the CdSe QDs (~80 nm) at the Au (Pd)/CdSe QDs interface can be calculated using Equation 4.8. Under zero bias condition, the widths of depletion region are found to be ~66 nm, and ~71 nm which cover nearly ~83% and

~89% of the CdSe QDs thin film (~80 nm) for Au and Pd based Schottky photodiodes respectively. Various device parameters of the two types of photodiodes investigated are listed in Table 6.1.

Table 6.1: Comparison among the CdSe Schottky diodes with Au and Pd electrode at room temperature.

Entities	**Au electrode**	**Pd electrode**
Built-in potential (V_{bi}, V)	0.54	0.41
Reverse saturation current (A)	1.89×10^{-8}	1.74×10^{-8}
Barrier height ($\phi_{B,eff}$, eV) calculated using J-V	0.76	0.76
Barrier height ($\phi_{B,eff}$, eV) calculated using C-V	0.82	0.82
Ideality factor, η_i	2.39	3.36
Carrier concentration (N_d, cm^{-3})	4.94×10^{16}	3.05×10^{16}
Depletion region (nm)	~66	~71

The electrical parameters in Table 6.1 clearly indicate the quality of the Au/CdSe QDs Schottky junction is comparable to Pd/CdSe QDs junction. However, the J-V characteristics in Figure 6.2 (a) and (b) show that the Pd/CdSe QDs based Schottky photodiode has better photoresponse than that of the Au/CdSe QDs based Schottky photodiodes which have been discussed below in details.

6.3.2 Photoresponse Characteristics

The transient photoresponse characteristics of the Schottky photodiodes under study have been analyzed using white LED light with output optical intensity of 96.8 $\mu W/cm^2$ at 500 nm. The LED light is controlled by using Arduino® microcontroller to achieve a pulsating light with an on-off period of 1 sec. The current density (J)

variations against time (sec) for the Au and Pd based devices have been shown in Figure 6.4 (a) and (b) respectively.

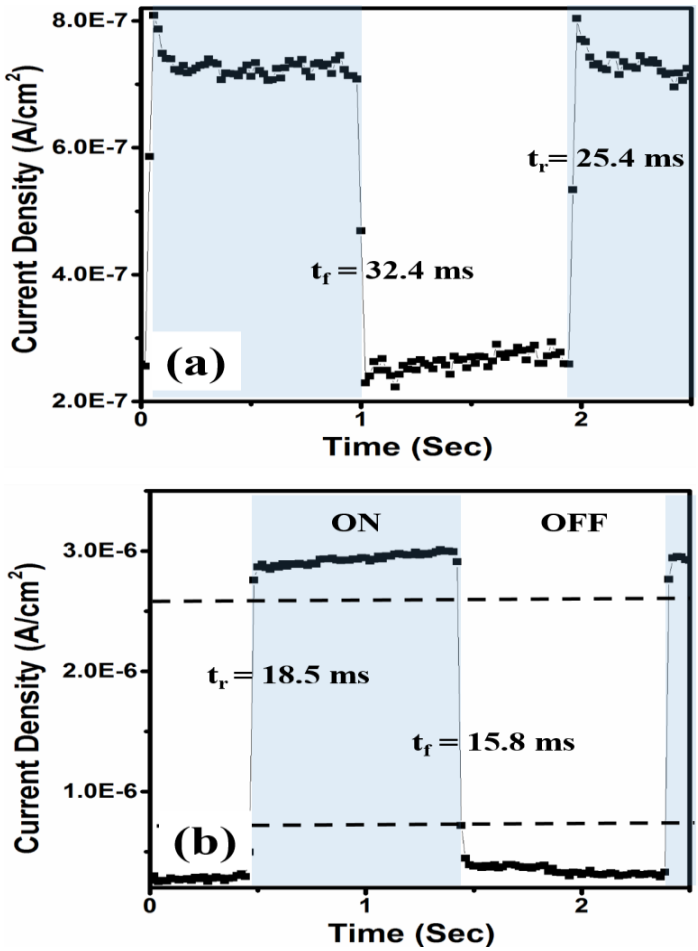

Figure 6.4: Time response characteristics of (a) CdSe QDs/ Au and (b) CdSe QDs/ Pd Self-powered Schottky photodiode under the pulsed illumination of white LED light controlled by using Arduino® microcontroller.

The overall response time (i.e. average of the rise time and fall time) of Pd/CdSe QDs is 17.15 ms (with rise time (t_r) of 18.5 ms and fall-time (t_f) of 15.8 ms) which is better than that of the Au/CdSe QDs based device with the overall response of 28.9 ms (with rise time (t_r) of 25.4 ms and fall-time (t_f) of 32.4 ms). The smaller built-in potential of Pd/CdSe QDs Schottky junction than that of the Au/CdSe QDs junction

listed in Table 6.1 justifies the faster response of the Pd based device of the Au based Schottky photodiodes.

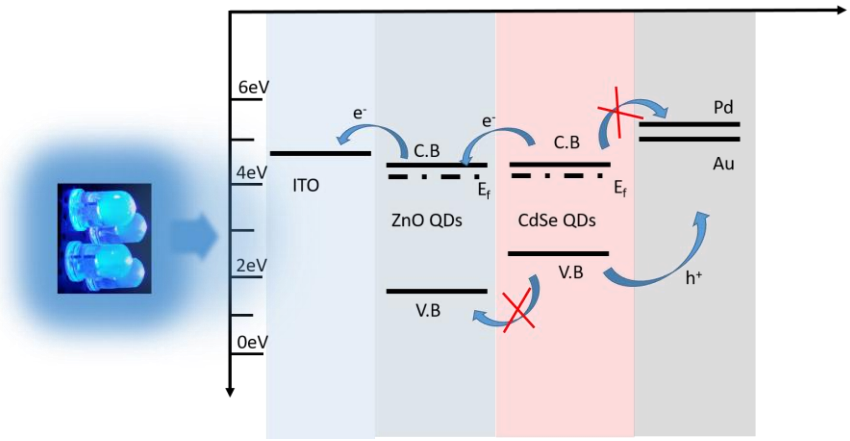

Figure 6.5: Schematic band diagram of ITO/ZnO QDs/CdSe QDs with Schottky contact.

The schematic band alignment diagrams of both the Schottky diodes have been shown in Figure 6.5 with the direction of incident illumination on the device. The fabricated Schottky diodes are illuminated from the back side (Glass/ITO side) to achieve the 100% illumination area. Note that the major portion of the light will be reflected back to open space from the metal surface if the device is illuminated from the top side as discussed in chapter 4. The ZnO QDs layer used in the device performs the following two major operations:

(i) It acts as the electron transport layer (ETL) in the device. The excess photo-generated electron-hole pairs in the active region (i.e., in the depletion region of the CdSe QDs layer) are drifted out due to the inherent electric field of the depletion region. The photogenerated electrons move towards ZnO QDs layer while the holes move towards the Au or Pd electrode. The use of ZnO QDs based ETL increases the photoresponse in multiple folds by extracting the majority of photogenerated electrons as discussed in chapter 4.

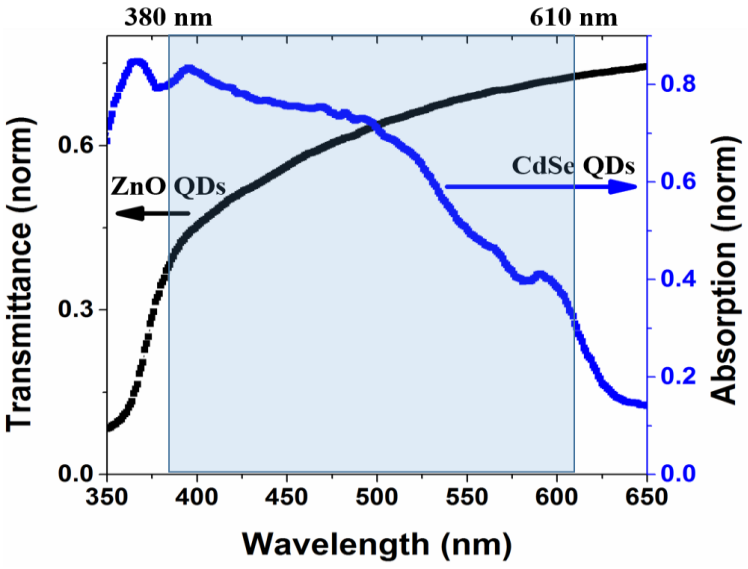

Figure 6.6: Transmittance of ZnO QDs thin film and Absorption of CdSe QDs plotted versus wavelength from 350 to 650 nm with the shaded active region of the device 380 to 610 nm.

(ii) The ZnO QDs layer deposited over the ITO coated glass substrate also acts as an optical filter for the PD operation. To establish it, the transmittance spectrum of ZnO QDs thin film is shown in Figure 6.6 along with the absorption spectrum of the CdSe QDs. The combined spectrum clearly shows that the lower limit of the operating wavelength (~380 nm) is determined by the ZnO QDs layer while the upper limit (~610 nm) is fixed by the absorption of the CdSe QDs. The light with wavelengths below 380 nm is absorbed by the ZnO QDs layer but do not contribute to the photocurrent of the device since it is located below the CdSe layer. Further, the responsivity *(R_e)*, detectivity *(D^*)* and external quantum efficiency *(EQE)* are the figure of merit parameters of the PDs calculated by using Equation 2.5, Equation 2.6, and Equation 2.7, respectively. The $R_e\ (\lambda,\ 0)$ and $J_{ph}\ (\lambda,\ 0)$ of the Au and Pd based Schottky photodiodes under study have been shown in Figure 6.7 (a) and (b) respectively. Note that the detectors under study are self-powered in nature since they possess significant characteristics of $R_e\ (\lambda,\ 0)$ and $J_{ph}\ (\lambda,\ 0)$ under zero applied bias condition (i.e. $V = 0$

volt). The detectivity, D^* *(λ, V)*, of a PD indicates the quality of PD to detect weak signals at wavelength λ and an applied bias of *V* volts.

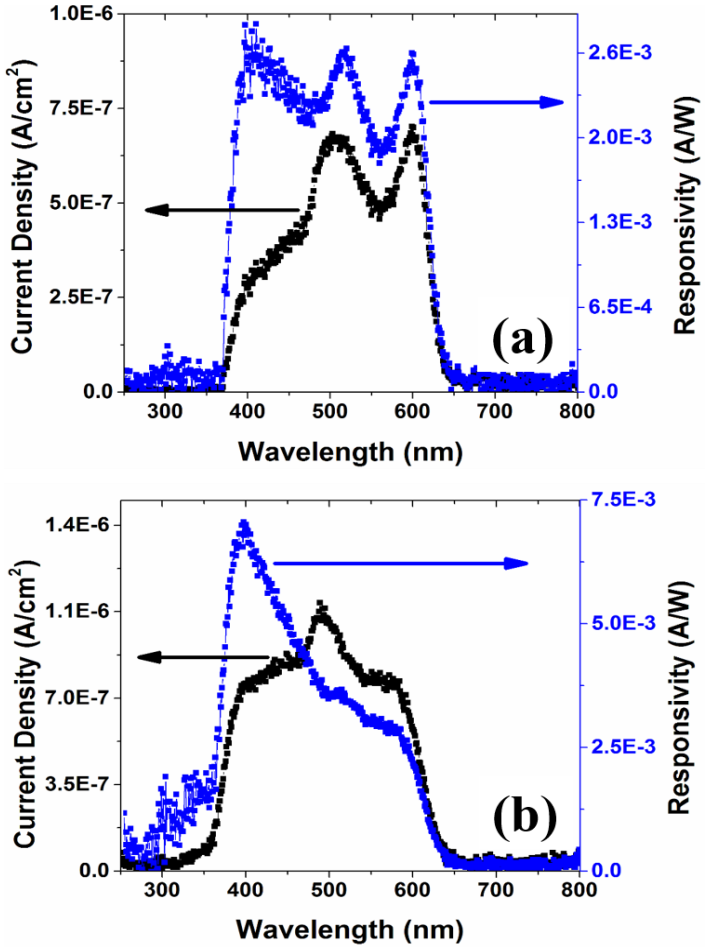

Figure 6.7: Current density and responsivity plotted against wavelength for Schottky diodes with (a) Au and (b) Pd electrode.

The *EQE* of the PD provides the percentage of total incident photons used to generate excess electron-hole pairs. The spectrums of *D* (λ, 0)* and *EQE (λ, 0)* of Schottky photodiodes with Au and Pd electrodes are shown in Figure 6.8 (a) and (b). We may observe from the figure that the lower limit (i.e. ~380 nm) of the spectrum is resulted from the transmittance spectrum of the ZnO QDs shown in Figure 6.6 while the upper limit (i.e. ~610 nm) of the spectrum is defined by the absorption characteristics of

the active layer, i.e. CdSe QDs which is also shown in Figure 6.6. The experimentally achieved spectrum of *D** and *EQE* is shown in Figure 6.8 are in trade with the overlapping area of transmittance of ZnO QDs and absorption of CdSe QDs shown as a shaded region in Figure 6.6.

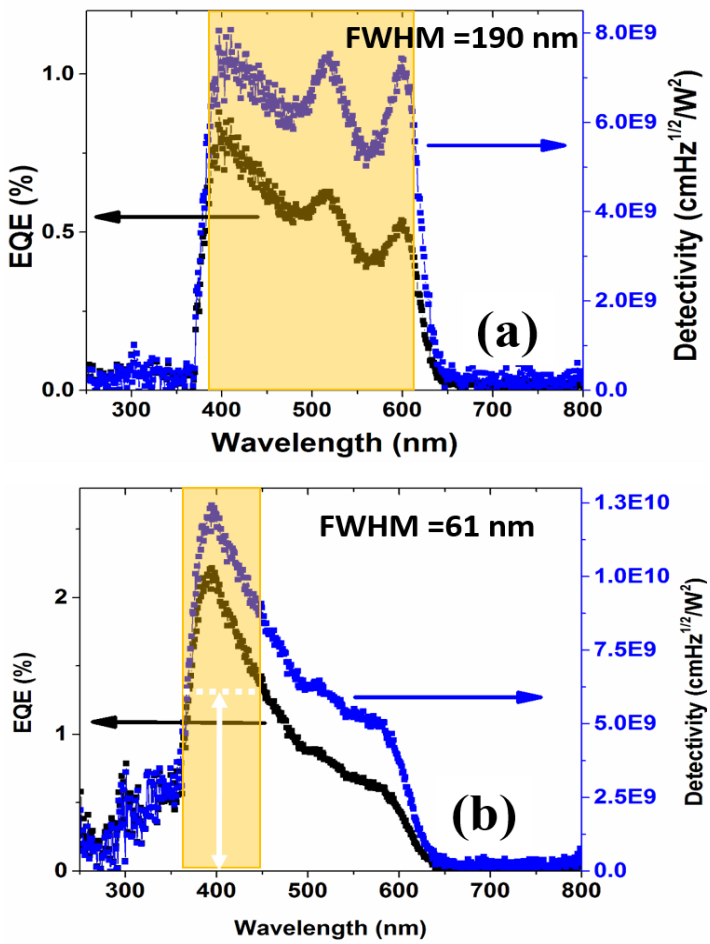

Figure 6.8: External Quantum Efficiency (EQE) and detectivity plotted against wavelength for Schottky diodes with (a) Au and (b) Pd electrode.

The Schottky diodes with Pd electrode possess much higher photoresponse than that of the Au electrode based devices. Further, the Pd electrode provides better selective photoresponse behavior with an FWHM of 61 nm as compared to the FWHM of 190 nm obtained for the Au based Schottky diodes. The results clearly show that the

Schottky metal electrode not only modifies the electrical properties but also affects the optical response of the device. To analyze further the effect of the electrode on the optical characteristics of the Schottky diode, we have developed the following theoretical analysis in support of the above observations.

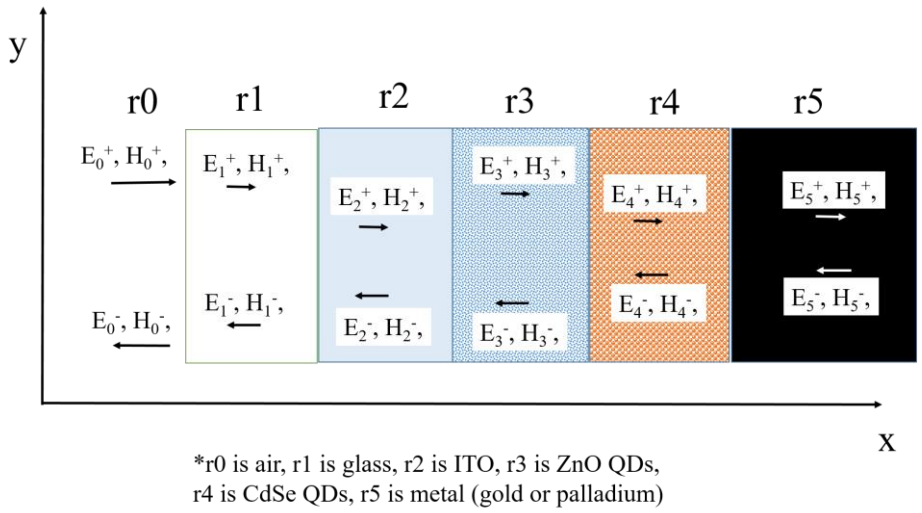

Figure 6.9: Incident field and reflected field depiction in each layer of the device under observation.

6.3.3 Theoretical Analysis

The different layers of the device under study have been shown in the Figure 6.9 for the incident electric field (E) and magnetic field (H)). The forward and backward propagating fields in the *x*-direction are indicated with the plus *(+)* and minus *(-)* signs respectively. The $E^{+/-}$ and $H^{+/-}$ field can be calculated using:(Hayt and Buck, 2006)

$$\left|E^2\right| = \frac{2P_{opt}}{cn\varepsilon_0} \tag{6.4}$$

where, P_{opt} is the incident optical power density measured using power meter (PM100D, Thorlabs) for different values of λ, c is the speed of light (3×10^{10} cm/sec), $\mathcal{E}_0$ is the vacuum permittivity (8.85×10^{-14} F/cm), and n is the refractive index of the thin films given by: (Hayt and Buck, 2006; Hamizi and Johan, 2012)

$$n = \frac{1+\sqrt{R}}{1-\sqrt{R}} \tag{6.5}$$

where, R is the reflectance of the film which can be measured by using Reflectometer (F-20, Filmetrics). Note that the forward and backward propagating fields depend on the interface of the different mediums. The reflected wave from the interface (backward propagating wave) is defined by the Reflection coefficient (Γ) while the transmitted wave from the interface (forward propagating wave) is defined by the Transmission coefficient (τ) calculated by using the following equations:(Hayt and Buck, 2006)

$$\Gamma = \frac{\eta_2 - \eta_1}{\eta_2 + \eta_1} \tag{6.6}$$

$$\tau = \frac{2\eta_2}{\eta_2 + \eta_1} \tag{6.7}$$

where η is the intrinsic impedance of the medium (1 and 2) accordingly. The intrinsic impedance of the medium can be calculated using:

$$\eta = \sqrt{\frac{j\omega\mu}{\sigma + j\omega\varepsilon'}} \tag{6.8}$$

where μ is the permeability and σ are the conductivity of the medium. Note that for ideal conductors, $\sigma \to \infty$ and hence $\eta \to 0$ (Equation 6.8). Solving Equation 6.6 and Equation 6.7 for $\eta_2 = 0$ leads to $\Gamma = -1$ and $\tau = 0$ *i.e.*, all the incident wave is reflected back, and none is transmitted. However, in practice, the conductivity of metals are finite. The conductivities of Pd and Au calculated from Hall measurements (HMS-3000, Ecopia) are 1.00×10^7 Ω^{-1}cm and 4.40×10^7 Ω^{-1}cm respectively. Permeability μ of the film is also calculated using:

$$\mu = \sqrt{\frac{n^2}{\varepsilon_r}} \tag{6.9}$$

$$\varepsilon_r = n^2 - k^2 \tag{6.10}$$

where k is the extinction coefficient calculated using absorption coefficient α as shown below: (Hamizi and Johan, 2012)

$$k = \frac{\alpha\lambda}{4\pi} \tag{6.11}$$

$$\alpha = 2.303\left(\frac{A}{d}\right) \tag{6.12}$$

$$A = 1 - (R + T) \tag{6.13}$$

where, A is the absorption of the thin film and T is transmittance of the thin film measured by using Reflectometer (F-20, Filmetrics). The reflection properties of metal/CdSe QDs interface depend on the type of the metal electrode (i.e., Au and Pd) while the reflection properties of the interfaces between different films are common in both the device structures under investigation. The normalized incident optical power at the metal/CdSe QDs interface measured over 350-650 nm (i.e., the spectrum of interest) by using a power meter (PM100D, Thorlabs) is shown as a shaded region in Figure 6.10 (a). The total transmitted and reflected powers are calculated at each of the interfaces of the ITO-coated-glass-substrate/ZnO QDs/CdSe QDs/metal (i.e., Pd or Au) structure assuming a back illumination from the substrate side (i.e., through the ITO-coated glass substrate). Further, the effect of reflected waves is also considered at every interface while calculating total power attenuated, transmitted or reflected by the film. The optical power absorption characteristics in the CdSe QDs (i.e., r4) layer due to the

forward propagating waves from r3/ r4 interface shown in Figure 6.9 are identical for both the Au and Pd based Schottky diode structures under study.

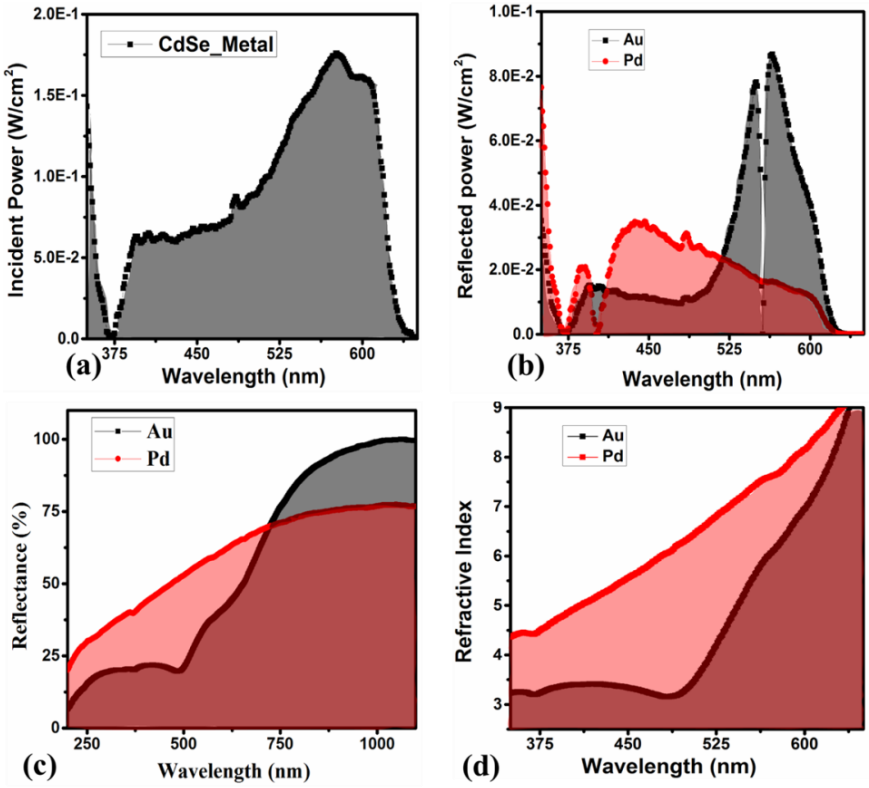

Figure 6.10: (a) Calculated incident power on the CdSe QDs/metal (Au or Pd) interface, (b) calculated total reflected power from the metal interface, (c) measured reflectance of Au and Pd thin films, and (d) calculated refractive index of Au and Pd thin films.

However, the total reflected powers from the metal/CdSe QDs interface are different for Au and Pd as shown in Figure 6.10 (b). The Pd/CdSe QDs interface reflects more optical power than that of Au/CdSe QDs interface in 400-500 nm region whereas the Au/CdSe QDs interface reflects more power as compared to Pd/CdSe QDs interface for 500 nm onwards. Note that the absorption spectrum of CdSe QDs starts at 610 nm and continuously increases towards shorter wavelengths as discussed in our earlier work(H. Kumar *et al.*, 2017). Clearly, the larger reflected optical power from the Pd/CdSe QDs interface than the Pd/CdSe QDs interface enhances the photoresponse of

the Pd based Schottky diodes multiple times of that of the Au/CdSe QDs based Schottky diodes. Note that the higher conductivity of Au than that of Pd should result in larger reflected power from the Au/CdSe QDs interface than the Au/CdSe QDs interface as discussed earlier. However, the measured reflectance characteristics of Au and Pd thin films shown in Figure 6.10 (c) give the opposite results. Figure 6.10 (c) shows that the Pd is more reflective for shorter wavelengths while the reflectance of the Au thin film is larger than the Pd thin film as we move towards higher wavelength (i.e., near-infrared or infrared) region. For 350-650 nm region, the reflectance of the Pd thin film is observed to be larger than that of the Au thin film in our study. The refractive indexes of the Au and Pd thin films calculated using Equation 6.5 are shown in Figure 6.10 (d). The results of Figure 6.10 (d) indicate that the speed of light in Pd thin film is very less as compared to the speed of light in the Au thin film. This implies that the backward reflection of optical light from the CdSe QDs/Pd interface will spend more time in the CdSe QDs layer which also confirms superior photoresponse of the Pd contact based Schottky photodiode over the Au contact-based device. The high reflected power from the Pd/CdSe QDs interface improves the overall responsivity, detectivity and quantum efficiency of the Schottky diode nearly three times of those of Au based Schottky photodiodes. Note that the active layer of CdSe QDs acts as an optical cavity in both the devices within which multiple reflections of light may take place from the metal (Pd, Au)/CdSe QDs and CdSe QDs/ZnO QDs interfaces. However, the higher reflection from the Pd/CdSe QDs layer increases the absorption of light in the active CdSe QDs layer by nearly three folds in the measured spectrum of 350-650 nm with respect to the Au based device. This optical cavity behavior results in the smaller FWHM value of 61 nm in case of Pd based device as compared to 190 nm of the Au

based device with enhanced of optical response as shown in Figure 6.8. It may be mentioned that the photoresponse parameters (i.e., responsivity, detectivity, and EQE) are normally decreased with the reduction in FWHM as reported by others (Qiao *et al.*, 2016). Thus, the enhanced photo-response with the reduced FWHM in the Pd/CdSe QDs based Schottky diodes under study differs from the traditional results for spectrum selective PDs.

6.4 Conclusion

This chapter reports the effects of the Schottky metal electrodes on the CdSe QDs layer on the characteristics of the metal/CdSe QDs/ZnO QDs/ITO based self-powered spectrum selective Schottky photodiodes for two Schottky metals Pd and Au. The colloidal QDs of ZnO and CdSe have been subsequently deposited on the ITO coated glass substrate by spin coating technique while the Pd or Au has been deposited on the active CdSe QDs layer by a thermal evaporation method. The effect of reflection from the metal (Pd, Au)/CdSe QDs interface on the optical cavity (i.e., CdSe QDs layer) formed between the ZnO QDs and the metal electrode (Au or Pd) are analyzed possibly for the first time in this chapter. The Pd electrode based photodiode shows nearly three times larger photoresponse (with responsivity (7.48 mA/W), detectivity (1.3×10^{10} $cmHz^{1/2}W^{-2}$), and EQE (2.21%)) as compared to those of the Au electrode based photodiode over a spectral range of ~380 nm to ~610 nm. The enhancement in the photoresponse for the Pd electrode based diode is attributed to the enhanced optical absorption in the active CdSe QDs layer due to larger reflection of light from the Pd/CdSe QDs interface than that from Au/CdSe QDs interface. Further, the Pd electrode based PD also shows a faster response (with a response time of 17.15 ms) than that of

the Au based PD (with the response time of 28.9 ms). The Pd based device shows a smaller FWHM of ~ 61 nm than ~190 nm FWHM value of the Au based device. The increased responsivity with decreased FWHM in the metal/CdSe QDs Schottky PDs is reported possibly for the first time in this chapter.